44th AIAA/ASME/ASCE/AHS Structures, Structural Dynamics, and Materials Conference , April 7-10, 2003. Norfolk, VA **AIAA-2003-1579**

SHAPE OPTIMIZATION FOR CONFORMING AIRFOILS

Shawn E. Gano * John E. Renaud † Stephen M. Batill † Andrés Tovar *

Department of Aerospace and Mechanical Engineering
University of Notre Dame
Notre Dame, Indiana
Email: John.E.Renaud.2@nd.edu

Abstract

Interest in the design and development of unmanned aerial vehicles (UAVs) has increased dramatically in the last two and a half decades. The Buckle-Wing UAV concept being developed in this research is designed to "morph" in a way which facilitates variations in wing loading, aspect ratio and wing section shapes. The Buckle-Wing consists of two highly elastic beam-like lifting surfaces joined at the outboard wing tips in either a pinned or clamped configuration. The Buckle-Wing UAV is capable of morphing between a separated wing configuration designed for maneuverability to a single fixed wing configuration designed for long range/high endurance. The design of the Buckle-Wing's aerodynamic shapes is critical to the functioning of this adaptive UAV airframe. The airfoils must be capable of functioning both as independent lifting surfaces and as a fused single wing. The adaptive airframe of the Buckle-Wing requires that the two airfoils/wings conform as one single wing for the extended range and/or endurance configuration. This paper is focused on the use of shape optimization technologies to optimally tailor the aerodynamic performance of the UAV airfoils in both the separated and single fixed wing configuration. A conforming multi-objective and multilevel airfoil shape optimization problem is formulated and solved. Given an exterior airfoil, optimized for long endurance, shape optimization can be used to decomposed the exterior airfoil into two conforming airfoils in such a way that when separated the airfoils produce a 85% increase in lift providing improved maneuverability.

Nomenclature

α	Angle of attack
ρ_∞	Free stream density
ω	Turning rate
c	Thrust-specific fuel consumption
c_d	Drag coefficient
c_l	Lift coefficient
D	Total drag
E	Endurance
g	Acceleration of gravity
L	Total lift
n	Wing load factor
r	Turning radius
R	Range
S	Planform Area
t	Time
V_∞	Free stream velocity
W	Weight of aircraft at any given time
W_1	Weight of aircraft without fuel and with full payload
W_o	Weight of aircraft with full fuel and payload

1 Introduction

There has been a growing interest in the development of unmanned arial vehicles (UAVs) for a variety of missions. These include video and IR surveillance, communication relay links, and the detection of biologi-

*Graduate Research Assistant, Student Member AIAA
†Professor, Associate Fellow AIAA.

cal, chemical, or nuclear materials. These missions are ideally suited to UAVs that are either remotely piloted or autonomous.

Unmanned aerial vehicles (UAVs) are an ideal application area for morphing aircraft structures. Existing fixed geometry UAV designs have generally been designed for maximum flight endurance and range to provide extended surveillance (i.e., single mission capability). Future classes of UAVs with morphing airframe geometries are envisioned for achieving both endurance and maneuverability in a single vehicle (i.e., multiple mission profiles).

A typical mission that a multi-role UAV could perform is depicted in Figure 1. This mission would include takeoff, cruise to some desired location as efficiently as possible, then it would encounter a flight situation in which high maneuverability is essential, then an efficient cruise back, and finally landing. In takeoff, high-g maneuvers, and landing, high lift is desired with much less emphasis on the level of drag. When cruising, however, maximum range/endurance is desired so the lift to drag ratio is important.

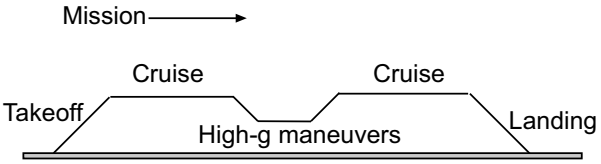

Figure 1. Typical mission scenario.

An adaptive airframe UAV concept that could accommodate such a versatile mission is a unique morphing UAV referred to as the Buckle-Wing, that is being developed at the University of Notre Dame. The wing consists of two highly elastic beam-like lifting surfaces joined at the outboard wing tips in either a pinned or clamped configuration. The UAV is capable of morphing between a separated wing configuration designed for maneuverability to a single fixed wing configuration designed for long range and/or high endurance.

The Buckle-Wing design has many advantages over a traditional UAV design because the trade off for maneuverability and range/endurance can be somewhat decoupled. Allowing the performance of each category to be greater than if a single design had them as competing objectives. With this new capability comes new design challenges. This paper addresses the airfoil shape optimization problem focusing mainly on the problem of conforming the high maneuverability airfoils into a fused single airfoil that exhibits high endurance characteristics.

In the following sections the Buckle-Wing UAV is described in greater detail, then a description of the fused and separated wing parameters are given. Third a trade study illustrates the different performances of the fused and separated wing configurations. The spacing between the separated airfoils is varied to illustrate the interaction effects. This is followed by developing the multiobjective and multilevel airfoil shape optimization problem. Two example problems and their solutions are presented and analyzed. The paper ends with some concluding remarks and future directions for the research.

2 The Buckle-Wing UAV

The morphing-wing UAV concept in development is the unique Buckle-Wing illustrated in Figures 2 and 3. This aircraft will be capable of independently changing wing loading, aspect ratio, and wing section shape while in flight.

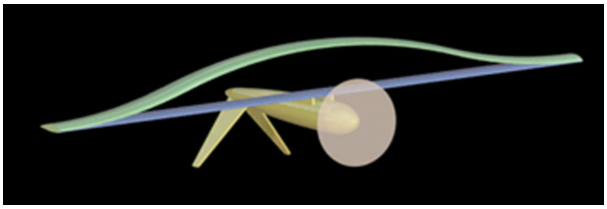

Figure 2. Buckle-Wing in separated configuration.

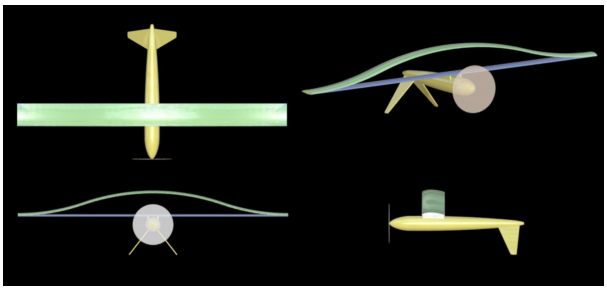

Figure 3. Buckle-Wing from different perspectives in separated configuration.

The Buckle-Wing consists of a lower lifting surface that is relatively stiff and an upper lifting surface with

outboard attachments to the lower wing and the capability of large, elastic-buckling deformations in pinned, clamped or various constrained sliding configurations. A variety of morphing deformations can be induced through controlled buckling of the elastic lift surfaces.

The buckle-wing acts as a fused single wing in the absence of applied buckling loads and morphs into vertically stacked wings when separated via application of controlled internal buckling loads. A variety of actuators exist for supplying/controlling the buckling loads. Outboard actuators can apply axial loads and a central actuator can apply a transverse load to separate the two lifting surfaces via buckling deformation, thereby providing the separated wing characteristic of decreased wing loading. Actuators in the wing-rib-structure can be used to attain smaller-scale deformations of the airfoil. The two wing surfaces will join to form a single wing with a much higher aspect ratio and increased wing loading in the absence of actuation forces.

2.1 Buckle-Wing Issues and Parameters

Airfoil design of the Buckle-Wing airfoils presents new challenges because of the fact that the separated airfoils have to conform into a single airfoil with optimal endurance performance characteristics. Issues that arise in this situation include how to determine the geometry of the fused airfoil and the separated airfoils. Can there be voids inside the mated configuration, and can flaps be used to smooth the joined leading edges.

Given an airfoil, there are many ways that the geometry could be parted or "cut" in order to give the most lift when the two smaller airfoils are separated. A few of the possibilities are depicted in Figure 4. In case (A) the cut runs from the bottom side of the airfoil and terminates near the trailing edge. This cut has a possible advantage in the fact that when the two smaller airfoils are separated the wings are staggered. This stagger can be beneficial to the lift generated as per a very early National Advisory Committee for Aeronautics report[14]. In case (B) of Figure 4 the airfoil is cut in some shape from the leading edge to the trailing edge resulting in both thinner airfoils having the same chord length as the original. In case (C) another possible cut, where just a thin cut from the top surface, not starting from the leading edge or ending at the trailing edge is proposed.

Most of the cuts proposed above prevent the shape optimization procedure from rounding the leading edges

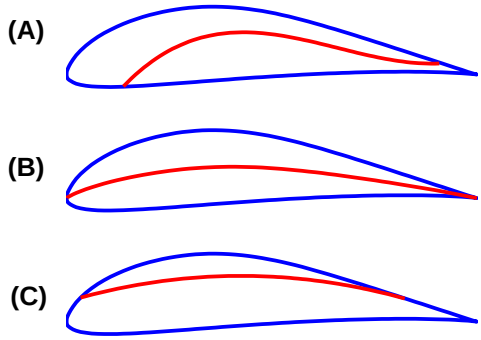

Figure 4. Possible conforming airfoil geometries.

of the separated airfoils. In addition, by cutting the airfoil we are artificially restricted to having a solid fused wing. To address the problem of not having rounded leading edges a mechanical flap may be considered for when the two airfoils mate, so that the fused shape also has a smooth continuous shape. If a highly cambered airfoil were to be mated to a lower less cambered airfoil this could cause a void within the fused shape. The presence of a void like this doesn't seem to pose any real problems as long as the fused shape is smooth and has a sharp trailing edge. These two issues are illustrated in Figure 5.

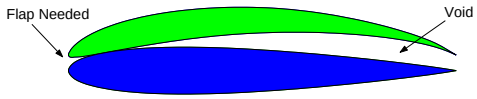

Figure 5. Conforming airfoils that have an internal void and a discontinuous leading edge.

Other variables that pertain to separated wings that are important to the design of the buckle-wing UAV include the wing separation distance and the wing stagger. The separation distance will vary from zero at the tips of the wing to some value at mid span. This spacing at mid span would effect the interference between the two airfoils as found in experiments on biplanes in the early half of the twentieth century[10,13] and in computational fluid dynamics simulations discussed in the next section. Structural issues are obviously very important in the design or the buckle-wing UAV. In this investigation structural design issues are not addressed.

3 Fused Versus Split Airfoil Trade Study

For an aircraft that is in cruise the main design goal is maximal range and/or endurance. For a jet powered air-

craft the Breguet equations give us an estimate for range and endurance and they are,

$$R = \frac{2}{c}\frac{c_l^{1/2}}{c_d}\sqrt{\frac{2}{\rho_\infty S}}(W_0^{-1/2} - W_1^{-1/2}) \tag{1}$$

and

$$E = \frac{1}{c}\frac{c_l}{c_d} ln\left(\frac{W_0}{W_1}\right). \tag{2}$$

From the endurance equation the only value we can control aerodynamically or improve via airfoil design is the lift to drag ratio. Thus in the design of the fused airfoil of the Buckle-Wing it is desirable to have the largest $\frac{c_l}{c_d}$. (For this paper we will focus on maximizing endurance, but the same method could be used for range or some trade-off between the two.)

Performance characteristics of an agile aircraft are a high turn rate and a small turning radius. Both are effected by the load factor, defined as,

$$n \equiv \frac{L}{W}. \tag{3}$$

Expressions for level turning radius and turn rate respectively are,

$$r = \frac{V_\infty^2}{g\sqrt{n^2-1}} \tag{4}$$

and

$$\omega = \frac{V_\infty}{r} = \frac{g\sqrt{n^2-1}}{V_\infty}. \tag{5}$$

Inspecting the maneuverability relations, it can be seen that the higher the load factor, *n*, the higher the turn rate is and the smaller the turning radius becomes. To improve the loading factor the weight of the aircraft should be kept as low as possible and the lift generated should be as high as possible. When the Buckle-Wing is in the buckled configuration it should have a high lift coefficient.

Table 1. Fused Airfoil

α	c_l	c_d	c_l / c_d
0	0.418	0.002	200.8
5	1.005	0.007	134.7
10	1.457	0.030	48.39

Table 2. Airfoil System Separated by 50% of cord

α	c_l	c_d	c_l / c_d
0	0.539	0.009	59.38
5	1.382	0.036	38.53
10	2.083	0.125	16.70

To investigate the effect of separating an airfoil into two smaller airfoils and to compare these trends with experimental biplane data, two dimensional CFD simulations were used. The CFD simulations were conducted for a fused case and then the airfoil was split slightly below the camber line and the simulations were repeated for three different separations (i.e. 10%, 25%, and 50% of the chord). Each of these cases were run for $\alpha = 0, 5$, and 10 degrees. The exterior airfoil shape used was the E-387[12,20]. The results are presented in Tables 1 and 2 for just the fused and 50% separated cases. The lift coefficient and lift to drag ratio for the three cases when $\alpha = 5$ is shown graphically in Figures 6 and 7.

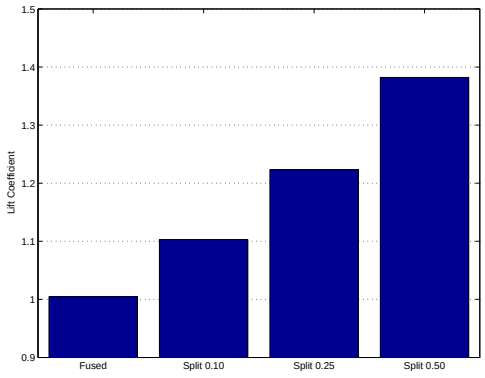

Figure 6. Lift coefficients for fused and various split configurations with angle of attack = 5 degrees.

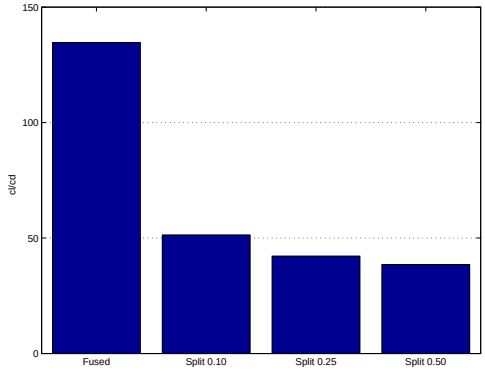

Figure 7. Lift divided by drag coefficients for fused and various split configurations with angle of attack = 5 degrees.

From Tables 1 and 2, and especially from Figures 6 and 7 it can be see that for the fused case the lift to drag ratio is much higher and when the airfoil is split the lift increases with increase in gap spacing. The non-dimensional coefficients, c_l and c_d, were calculated using the same unit length (chord = 1) in both the fused and separated cases. This was done so that the comparison of values between the cases would be consistent. From this we can conclude, at least in this example, that the Buckle-Wing approach could indeed provide for a multi-role UAV. Similar trends can be found in the NACA biplane literature [14,13,10], which also gives some verification that the analysis used in this study can predict the approximate behavior associated with the interference between the separated airfoils.

FUN2D was the CFD code used for analysis this program and the settings used are discussed in greater detail in section 5.

4 Full Design Problem Description

As stated in the previous section the multiobjective optimization seeks to find an exterior airfoil that maximizes high endurance performance, that can be decomposed into two airfoils, that when separated produce maximum high lift performance for maneuverability. This is posed as a multiobjective and multilevel optimization problem for determining the buckle-wing UAVs conforming airfoils.

A flowchart of the optimization problem is shown in Figure 8. The system level optimizer varies the geometry of the fused airfoil (external geometry) and the angle of attack for the fused deployment to achieve the highest endurance (c_l/c_d maximum) for the fused shape, and the most maneuverable (c_l maximum) separated configuration. For each iteration the performance of the fused airfoil is computed and then the geometry is input to a sublevel optimization problem that finds the optimal separated airfoil geometries for maneuverability. The sublevel optimization is solved for the current exterior airfoil iterate. In this sub optimization problem the angle of attack of the UAV, when in the separated configuration, is also determined. The optimal value of c_{lmax} is found and then passed back to the system level. This is a multi-objective, multi-level optimization formulation.

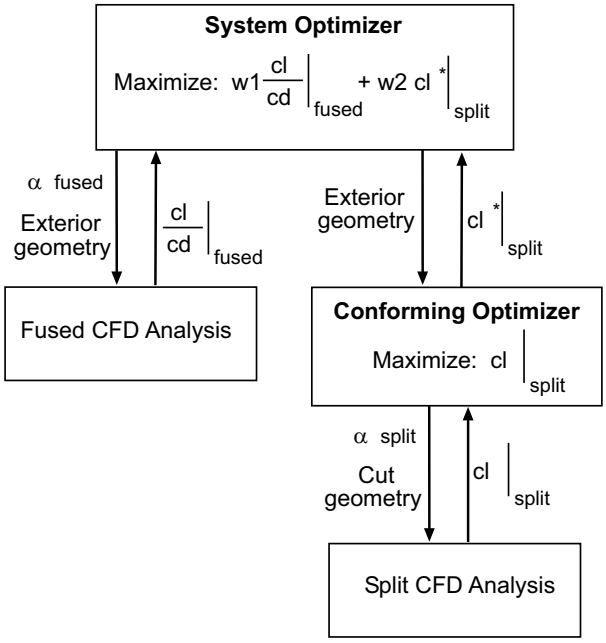

Figure 8. Flowchart for the conforming airfoil optimization framework.

The flowchart in Figure 8 doesn't show the constraints that are imposed on the system. For the system level optimization there is a constraint on the lift coefficient that must minimally be produced by the fused airfoil, along with other possible aerodynamic constraints that may be desired. Structural constraints must also be enforced so that the airfoils don't become too thin. In the sub optimization problem, there are again general aerodynamic constraints and structural constraints. A minimal lift to drag ratio can also be used as a constraint.

The two airfoil configurations do compete because their geometries must conform with one another. Weights, w_1 and w_2, are added to the objective function so that the designer can control the importance of each objective.

The mathematical optimization statement can be posed as,

$$\begin{aligned} \underset{\mathbf{x}}{\text{maximize :}} \quad & w_1 \left.\frac{c_l}{c_d}\right|_{fused} + w_2 \left. c_l^* \right|_{split} \\ \text{subject to :} \quad & \mathbf{l} \leq \begin{pmatrix} \left. c_l \right|_{fused} \\ \mathbf{Aero}(\mathbf{x}) \\ \mathbf{Struct}(\mathbf{x}) \\ \mathbf{x} \end{pmatrix} \leq \mathbf{u}. \end{aligned}$$

Where $\left. c_l^* \right|_{split}$ is the optimal value of the sub optimization airfoil conforming problem,

$$\begin{aligned} \underset{\mathbf{x}_{sub}}{\text{maximize :}} \quad & \left. c_l \right|_{split} \\ \text{subject to :} \quad & \mathbf{l} \leq \begin{pmatrix} \left.\frac{c_l}{c_d}\right|_{split} \\ \mathbf{Aero}(\mathbf{x}_{sub}) \\ \mathbf{Struct}(\mathbf{x}_{sub}) \\ \mathbf{x} \end{pmatrix} \leq \mathbf{u}. \end{aligned}$$

The design variables for the main optimization consist of a parametrization of the fused geometry and its angle of attack. Further design variables are introduced in the sub problem and they consist of the airfoil parting geometry and the angle of attack for the craft in the buckled configuration.

The sub optimization problem was used instead of letting the system level optimizer handle all of the design variables because this insured a continuous design space. If the system level optimizer could change the cut and the fused shapes, then it would be possible that the shape of the cut would in fact not fit within the shape of the fused airfoil. If this occurred then there would be no way to perform the CFD analysis because the geometry would be not possible. It would be possible to set constraints on these shapes but this would be difficult to do using the methods of parametrization used (basis functions) to express the shape of the fused airfoil. If splines were used for describing both geometries then this problem could be written with a single level optimization, however there would need to be many control points on the surface and thus many design variables and therefore making the problem quite computationally expensive. Other methods are possible to rewrite this problem as a single level optimization but make the design space very complex. So at this stage in the research it has been decided to keep the coupling of the two optimizations separate.

The methods used to parameterize the geometry of both the fused shape and the cut play a large role in the computational expense of this optimization. Also the method used to calculate gradients of the objective function is important. Both are discussed in the next two subsections.

4.1 Geometric Parametrization

The way in which the geometry of the fused airfoil and the cut are parameterized is important because it effects the number of design variables in the system and the shape possibilities. As the number of design variables increases the optimization algorithm needs more data especially in the form of gradients for each variable. Because CFD is very expensive this information is quite time consuming to calculate. On the other hand the more values used to describe the shape of these two geometries the greater the freedom the optimizer has to find the best possible shape. Two different methods have been used to describe the geometries. For the fused airfoil, basis functions were used and for the cut, cubic splines were used.

An approach used by Vanderplaats[21], called basis functions, was used to describe the fused airfoil shape. The method uses a set of airfoil geometries as a basis for creating new geometries. Design variables are used for the various weights of each of the basis shapes. Each of these weights are multiplied by their respective airfoil and then these shapes are summed up to form a new shape. Because all of the airfoils are smooth the resultant shape is guaranteed to be smooth and to have the appropriate characteristics, such as a rounded leading edge and a sharp trailing edge. This approach is preferred over using spline control points because it requires less design variables to make new airfoil shapes. However splines do have the capability of making any possible shape where the basis functions may not.

The cut shape could be described in terms of basis shapes as well. One approach would be to use a set up upper surfaces and lower surfaces as the basis. However in the test cases presented in this paper spline control points are used to vary the shape of the cut. This was done in order to see what general shapes would be found

for the cut and not to bias it with a small set of possible basis shapes.

4.2 Sensitivity of the Sub Optimization Problem

The objective function of the system optimization contains the result of the sub optimization. For gradient based methods this would result in calculating the gradient of an entire optimization. This optimization is very expensive so finite differencing is not practical. Thus post optimality analysis should be exploited.

A post optimality relation based on the first order Kuhn-Tucker optimality conditions is [19],

$$\frac{dc_l^*}{dx_i} = \frac{\partial c_l}{\partial x_i} + \sum_j u_j \frac{\partial(-g_j)}{\partial x_i}. \qquad (6)$$

Where u_j are the Lagrange multipliers, g_j are the inequality constraints, and x_i are the design variables of the system level optimizer. Only the active constraints are considered in Equation 6.

5 Example Problems

The work presented in this paper details the preliminary results of this investigation. The two examples in this section solve the sub optimization problem or the problem that deals with cutting a given shape optimally for maneuverability when the airfoils are separated. This is the bulk of the new concepts presented here since standard airfoil optimization has been studied extensively in the past and still continues to be an important research topic[16]. Methods such as airfoil design under uncertainty and robust design are also issues that can be added to this problem[9]. In the first example, a given airfoil is cut to maximize lift with just geometric design variables. In the second example the problem remains the same except the angle of attack is also added to the design variable set. Implementation of the multilevel multiobjective optimization are currently in progress.

5.1 Problem Specifics

In each test case the fused shape was given. This shape was the E-387. The cut was parameterized by 3 control points and 3 fixed nodes all fitted with a cubic spline curve. The three fixed nodes included one at the leading edge, one at the trailing edge and one near the trailing edge to insure that each split airfoil had a sharp trailing edge. The top of Figure 9 shows the shape of the airfoil in its fused shape with the cubic spline and control points along the camber line. Also in Figure 9 the general shape of the split airfoils are given for the starting point and optimized shape so that the optimization process is easier to visualize.

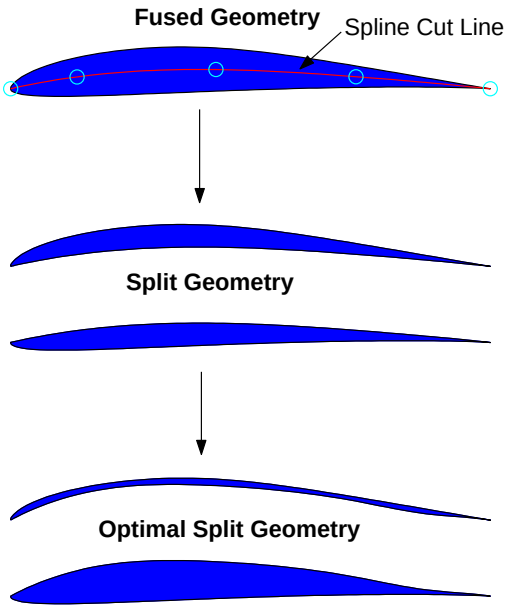

Figure 9. Conforming airfoil optimization geometries.

The design variables, **x**, for these two cases include three vertical displacements of the cubic spline nodal points and in the second case the angle of attack is added. The vertical displacements are referenced from the camber line. The angle of attack is only for the separated configuration.

In both cases the objective function and constraints were,

$$\begin{aligned} &\text{maximize}: \quad c_l|_{split} \\ &\quad \mathbf{x} \\ &\text{subject to}: \\ &\begin{pmatrix} 20 \\ -0.0267 \\ -0.0299 \\ -0.0148 \\ 0 \end{pmatrix} \leq \begin{pmatrix} c_l/c_d \\ x_1 \\ x_2 \\ x_3 \\ \alpha \end{pmatrix} \leq \begin{pmatrix} \infty \\ 0.0267 \\ 0.0299 \\ 0.0148 \\ 10^o \end{pmatrix}. \end{aligned}$$

Where α is only implemented in case 2. The bounds on the design variables, x_1 to x_3, represent points that are 35% of the local airfoil thickness above and below the camber line. This could result in thin airfoils and could be adjusted based on structural information if desired.

For both cases the Reynolds number was one million, the Mach number was 0.35. An unstructured grid was used that consisted of 60,000 elements and extended to 30 times the cord in each direction. The grid around the airfoils can be seen in Figure 10 for the starting cut. The turbulence was modelled with the k-ω model. The flow solution was accelerated using a multi-grid scheme consisting of the fine mesh and one with half as many grid points.

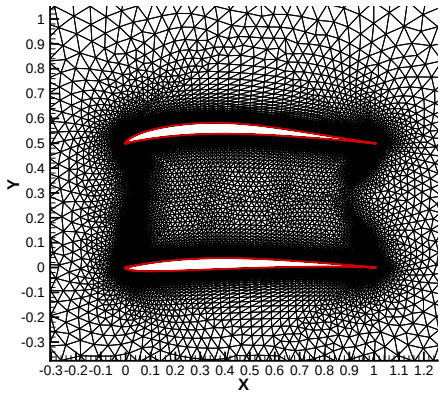

Figure 10. Unstructured mesh around the separated airfoils.

The FUN2D (Fully Unstructured Navier-Stokes in 2D) code was used for the CFD analysis. The code was developed by NASA at the Langley Research Center[3,4].

The optimization was performed using MATLAB's optimization toolbox's fmincon. The optimizer uses a Sequential Quadratic Programming (SQP) method. In this method, a Quadratic Programming (QP) subproblem is solved at each iteration. An estimate of the Hessian of the Lagrangian is updated at each iteration using the BFGS formula[11]. The starting point was zero for the three shape variables and 2 degrees for the angle of attack used in case 2. The results are discussed in the following sections.

Table 3. Results of Case 1 Optimization fixed α

	Starting Design	Optimal Design
x_1	0	0.0185
x_2	0	0.0299
x_3	0	0.0148
c_l	0.954	1.024

5.2 Case 1 Results: Fixed Angle of Attack

The optimization of the cut of the fused geometry to produce the most lift took 6 iterations. The starting lift coefficient was 0.954 and the final value was 1.024. For reference the fused airfoil in this case had a lift coefficient of 0.635. Table 3 lists the starting and optimal values for the design variables and the objective function.

The results show that all but the first design variable were at their upper bounds and the first one was not too far from this bound. Figure 11 shows the contours of the Mach number around the separated airfoils and the optimal geometry.

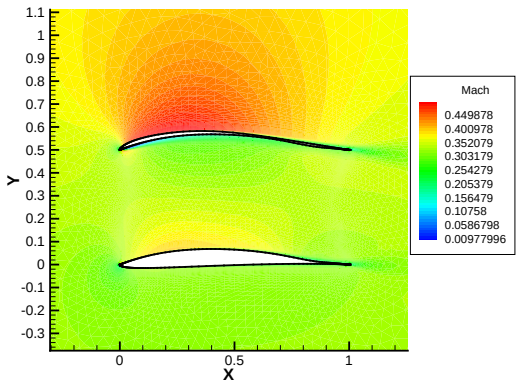

Figure 11. Mach contours for case 1 optimal design

5.3 Case 2 Results: With Angle of Attack

Optimizing the same problem but including the angle of attack as a design parameter also took 6 iterations. In this case the objective function more than doubled after optimization. Table 4 lists the starting and optimal

Table 4. Results of Case 2 Optimization with α

	Starting Design	Optimal Design
x_1	0	0.0267
x_2	0	0.0299
x_3	0	0.0134
α	2	8.75
c_l	0.954	2.12

values for the design variables and the objective function.

Again the values of two of the design variables reached their upper bounds. In this case x_2 was slightly below it's upper bound. In Figure 12 the design variable values are plotted versus iteration number and in Figure 13 the objective function value is shown versus iteration.

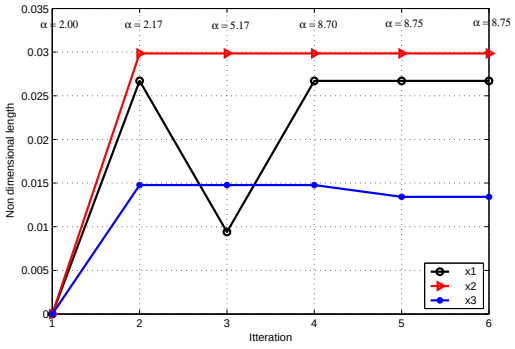

Figure 12. Design variable values versus iteration.

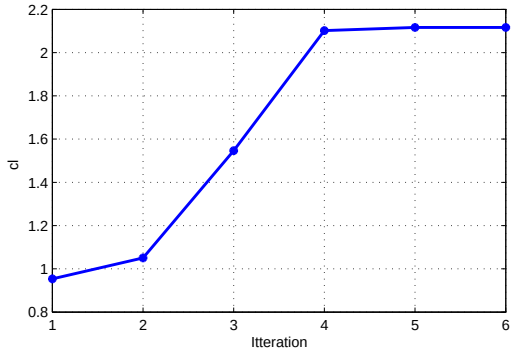

Figure 13. Objective function history.

The angle of attack did not go to its upper bound. Figure 14 shows the Mach contours of this solution.

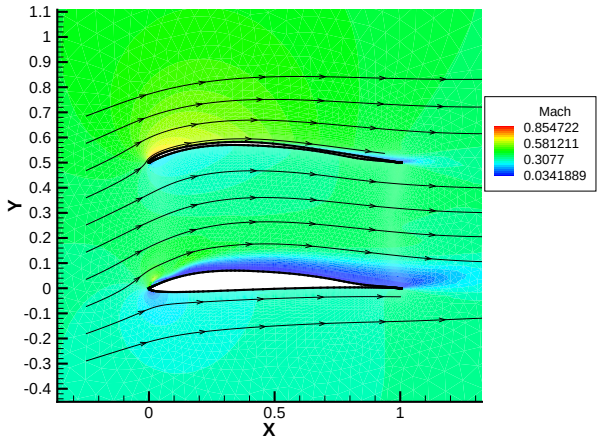

Figure 14. Mach contours and stream lines for case 2 optimal design.

6 Conclusions Future Work

The results of the two conforming airfoil shape optimization examples, illustrate the potential benefit of the buckle-wing UAV. The optimized cut allows the separated airfoils to produce greater lift which facilitates an increase in maneuverability of the system. Thus, an UAV could be optimized for a multi-mission role that included both maneuverability and long range / high endurance, without having to compromise as much between the two different performance criterion. Current efforts are focused on performing the multi-objective and multilevel optimization described in section 4.

Another observation that can be made from the results of the test cases is the fact that the geometry of the cut tended to create as thin of an upper airfoil as possible. When optimizing the entire system this fact could allow the lower level optimization to converge faster by starting from a point that is close to the geometric upper bound.

In future research different methods of cutting the wing should be explored. The ability to cut the airfoil in different ways could be beneficial. Running the entire system optimization is computationally expensive so parallelization of the code is another future goal. Inclusion of structural performances and constraints will also be important in designing the Buckle-Wing UAV.

Acknowledgments

This research effort is supported in part by the following grants and contracts: ONR Grant N00014-02-1-0786 and NSF Grant DMI-0114975. We would also like to express our thanks to Eric Nielsen of NASA's Langley Research Center for answering many questions regarding the FUN2D software.

References

1. Abbott, I.H., Von Doenhoff, A.E.: *Theory of Wing Sections*, Dover, 1959.

2. Anderson, J.D.: *Introduction to Flight*, McGraw-Hill, 1989.

3. Anderson, W.K., Bonhaus, D.L.: *An Implicit Upwind Algorithm for Computing Turbulent Flows on Unstructured Grids*, Computers and Fluids, Vol. 23, No. 1. pp. 1-21, 1994.

4. Anderson, W.K., Rausch, R.D., Bonhaus, D.L.: *Implicit/Multigrid Algorithms for Incompressible Turbulent Flows on Unstructured Grids*, AIAA 95-1740, J. Comp. Phys. Vol. 128, 1996, pp. 391-408.

5. Belegundu, A.D., Chandrupatla, T.R: *Optimization Concepts and Applications in Engineering*, Prentice Hall, 1999.

6. Corke, T.C.: *Design of Aircraft*, Prentice Hall, 2003.

7. Fletcher, C.A.J.: *Computational Techniques for Fluid Dynamics*, vol 1, Springer, 1991.

8. Fletcher, C.A.J.: *Computational Techniques for Fluid Dynamics*, vol 2, Springer, 1991.

9. Huyse, L., Padula, S.L., Lewis, R. M., Li, W.: *A probabilistic approach to free-form airfoil shape optimization under uncertainty.* AIAA Journal, Vol. 40, No. 9, September 2002, pp. 1764-1772.

10. Knight, M., Noyes, R.W.: *Wind Tunnel Pressure Distribution Tests on a Series of Biplane Wing Models Part II. Effects of Changes in Decalage, Dihedral, Sweepback and Overhang*, National Advisory Committee for Aeronautics Report No. 325, 1929.

11. The Mathworks Inc.: *Optimization Toolbox User's Guide Version 2.1*, 2002.

12. Miley, S.J.: *A Catalog of Low Reynolds Number Airfoil Data For Wind Turine Applications*, February 1982.

13. Munk, M.M.: *General Biplane Theory*, National Advisory Committee for Aeronautics Report No. 151, 1923.

14. Norton, F.H.: *The Effect of Staggering A Biplane*, National Advisory Committee for Aeronautics Report No. 70, 1921.

15. Padula, S.L., Rogers, J.L., Raney, D.L.: *Multidisciplinary Techniques and Novel Aircraft Control Systems*, 8th AIAA/NASA/USAF/ISSMO Multidisciplinary Analysis and Optimization Symposium, Long Beach, California, AIAA 2000-4848, September 6-8, 2000, pp. 11.

16. Padula, S.L., Li, W.: *Options for robust airfoil optimization under uncertainty.* Presented at Ninth AIAA/USAF/NASA/ISSMO Symposium on Multidisciplinary Analysis and Optimization, September 4-6, 2002. also AIAA 2002-5602.

17. Pérez, V. M., Renaud, J.E., Watson, L. T.: *Adaptive Experimental Design for Construction of Response Surface Approximations*, Proceedings of the 42st AIAA/ASME/ASCE/AHS/ASC Structures, Structural Dynamics, and Materials Conference, AIAA 2001-1622, Seattle, WA, April 16-19, 2001.

18. Ravindra V.T., Renaud, J.E., Rodríguez, J.F.: *An Interactive Multiobjective Optimization Design Strategy For Decision Based Multidisciplinary Design*, Engineering Opitmization, 2002, Vol. 34(5), pp. 523-544.

19. Renaud, J.E.: *Using the Generalized Reduced Gradient Method to Handle Equality Constraints Directly in a Multilevel Optimization*, Master of Science Thesis, Rensselaer Polytechnic Institute, 1989.

20. Selig, M.S., Donovan, J.F., Fraser, D.B.: *Airfoils at Low Speeds*, Soartech 8 H. A. Stokely, 1989.

21. Vanderplaats, G.N.: *Numerical Optimization Techniques for Engineering Design*, McGraw-Hill, 1984.

22. Wlezien, R.W., Horner, G.C., McGowan, A.R., Padula, S.L., Scott, M.A., Silcox, R.J., Simpson, J.O.: *The Aircraft Morphing Program*, 39th AIAA/ASME/ASCE/AHS/ASC Structures, Structural Dynamics, and Materials Conference, Long Beach, California, AIAA 98-1927, April 20-23, 1998.